



**HAL**  
open science

# DYNAMIC FRACTURE PROPERTIES OF A TUNGSTEN, 3.5% Ni, 1.5% Fe ALLOY UNDER EXPLOSIVE LOADING CONDITIONS

W. Reid, B. Walsh

► **To cite this version:**

W. Reid, B. Walsh. DYNAMIC FRACTURE PROPERTIES OF A TUNGSTEN, 3.5% Ni, 1.5% Fe ALLOY UNDER EXPLOSIVE LOADING CONDITIONS. *Journal de Physique IV Proceedings*, 1991, 01 (C3), pp.C3-597-C3-604. 10.1051/jp4:1991384 . jpa-00250529

**HAL Id: jpa-00250529**

**<https://hal.science/jpa-00250529>**

Submitted on 4 Feb 2008

**HAL** is a multi-disciplinary open access archive for the deposit and dissemination of scientific research documents, whether they are published or not. The documents may come from teaching and research institutions in France or abroad, or from public or private research centers.

L'archive ouverte pluridisciplinaire **HAL**, est destinée au dépôt et à la diffusion de documents scientifiques de niveau recherche, publiés ou non, émanant des établissements d'enseignement et de recherche français ou étrangers, des laboratoires publics ou privés.

**DYNAMIC FRACTURE PROPERTIES OF A TUNGSTEN, 3.5% Ni, 1.5% Fe ALLOY UNDER EXPLOSIVE LOADING CONDITIONS**

W.D. REID and B.E. WALSH

*DSTO, Materials Research Laboratory, P.O. Box 50, Ascot Vale, Victoria 3032, Australia***RESUME :**

La fragmentation naturelle et la fracturation de cylindres creux en alliage de tungstène (95% W, 3,5% Ni, 1,5% Fe) remplis d'un explosif, ont été analysées par le biais d'une étude paramétrique sur les dimensions caractéristiques des cylindres. On observe que le rapport masse/nombre des fragments suit une loi bilinéaire conforme à la relation de Payman modifiée. La classification dimensionnelle des fragments constitue une base de données pour l'étude du mode de fragmentation de systèmes rainurés à base de cet alliage.

**Abstract** - The natural fragmentation and fracture characteristics of a tungsten alloy (95%W,3.5%Ni,1.5%Fe) are evaluated using hollow, explosive-filled cylinders whose dimensions are varied systematically. Fragment mass/number distributions are found to conform to a dual slope linear fit to the modified Payman distribution. Fragment classifications and measurements are used to determine baseline data for efficient design of notching systems to control the breakup of casings made from this alloy into fragments of preferred size.

**1. INTRODUCTION**

The requirement for increased performance of military weapons has led to the use of specialised alloys in armour-piercing and fragmenting projectiles. Alloys of depleted uranium and tungsten are commonly used in kinetic energy penetrators to defeat advanced armours. Tungsten alloys are increasingly used in fragmenting munitions such as missile warheads and gun-launched projectiles [1].

Typically, these munitions incorporate compact, pre-formed tungsten alloy fragments. Although the manufacture of tungsten cubes or spheres is relatively simple, the assembly of the fragments into the munition is relatively complex and costly. In other munitions, controlled fragmentation techniques, using various notching patterns, are used to produce fragments of preferred size from a monolithic casing [1].

The present study examines the natural fragmentation of a tungsten alloy commonly used in munitions - 95%W, 3.5%Ni, 1.5%Fe. The aims were firstly, to provide a data base for the design of optimum techniques for achieving controlled fragmentation. Secondly, it was considered feasible that cost-effective munitions incorporating naturally fragmenting casings

may be suitable for some applications, particularly where mechanical notches are unacceptable because of the reduced structural integrity of the casing that this causes.

## 2. EXPERIMENTAL

A total of 21 right cylinders were machined from sintered tungsten cylindrical blanks having a nominal composition of (wt.%) 95W, 3.5Ni, 1.5Fe. The density of the blanks was 17.2 Mg/m<sup>3</sup>. All cylinders were ultrasonically inspected after machining to ensure freedom from significant voids or other flaws. No post-sintering heat-treatments were employed.

The dimensions and C/M ratios of the cylinders are shown in Table 1. The cylinder sizes were varied systematically in two ways. Firstly, all dimensions were increased proportionately resulting in cylinders of increasing wall thickness and diameter but constant explosive charge mass to cylinder mass (C/M) ratio. Second, cylinder dimensions were varied to produce cylinders of fixed wall thickness (4.5 mm), but increasing C/M ratio. Triplicate tests were conducted for each test cylinder geometry.

Table 1

Dimensions and Charge/Mass Ratios of Tungsten Alloy Cylinders

Cylinder size no.	O.D. (mm)	I.D. (mm)	Wall (mm)	Length (mm)	C/M ratio
1	65.0	49.0	8.0	130	0.12
2	48.7	36.7	6.0	100	0.12
3	36.6	27.6	4.5	100	0.12
4	24.4	18.4	3.0	100	0.12
5	60.5	51.5	4.5	120	0.24
6	48.6	39.6	4.5	100	0.18
7	24.3	15.3	4.5	100	0.06

Full recovery fragmentation tests were performed using cylinders filled with Composition B explosive (55% RDX, 44% TNT, 1% Beeswax). A 25 mm lead-in and a 6 mm lead-out were used on all charges to minimise end effects. The charges were directly initiated by exploding bridge wire detonators while the cylinders were located in a water filled pit. The mass of fragments recovered in each of the tests after removal of the water from the pit was approximately 97%. Fragments were then sorted and weighed using standard techniques [2].

Fragment mass/number distributions were analysed using a length modified Payman plot [3]. This is achieved by plotting Log P (where P is the cumulative percent mass of fragments with mass greater than M) against  $M/M_0$  (where M is the fragment mass and  $M_0$  the test cylinder mass). The slope of the straight line fit to this plot is designated the Modified Payman Fragmentation Parameter  $C_0^*$ . This parameter must then be divided by the cylinder length (L) to give the Length Normalised Payman parameter ( $C_L$ ), which is a measure of the coarseness of fragmentation.

The fragment morphology was characterised using visual and low-power optical examination of the fragment shapes and fracture types. Microstructural features were examined using conventional metallographic techniques. Microscopic fracture surface features were examined using a Scanning Electron Microscope (SEM).

### 3. RESULTS AND DISCUSSION

#### 3.1 Fragment Mass Distributions

A typical modified Payman plot for the tungsten alloy cylinders is shown in Fig.1 below. With ferrous alloys, a straight line fit to the modified Payman plot is normally obtained. However, for all tungsten alloy cylinders there was a distinct change in the slope of the plot approximately mid-range on both axes. The curve of best fit consisted of two straight lines of different slope which intersected at a point defined as the slope change point (SCP).

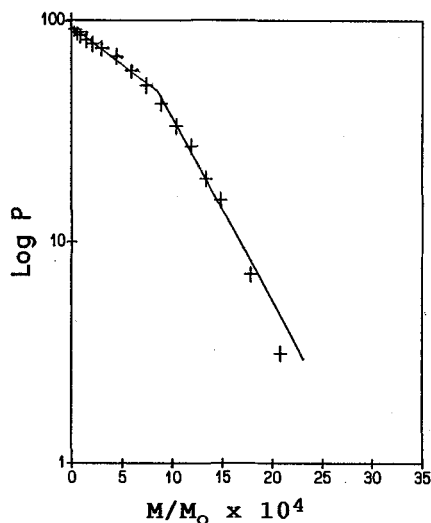


Fig.1 Typical modified Payman fragment mass/number distribution for Tungsten Alloy Cylinder Size Number 1.

For all cylinders, normalized Payman parameters ( $C_L$ ) were determined for the two parts of the modified Payman mass/number distributions. Parameters determined for the fragments with masses less than and greater than that of the SCP were defined as Range 1 and Range 2 parameters respectively.

In general terms, the  $C_L$  values obtained for the tungsten alloy cylinders tested were extremely high (fine fragmentation) [4]. For example the fragment mass/number distributions were about an order of magnitude finer than those produced by cylinders made from medium carbon steels, and about 50% finer than Spheroidal Graphite cast iron [5].

Fragmentation parameters ( $C_L$ ) determined for both Ranges 1 and 2

showed a small decrease with increasing cylinder wall thickness (0.12 C/M ratio). This trend is illustrated in Fig.2(a) for fragments from Mass Range 1 only (Note a linear fit is not used, as extrapolation will result in a zero value for  $C_L$  at an unrealistic wall thickness value). However,  $C_L$  values determined for fragments from both Mass Ranges 1 and 2 showed a large increase with increasing C/M ratio (4.5 mm wall thickness). This trend is illustrated in Fig.2(b) for Mass Range 1 fragments.

This behaviour can be understood in terms of the fracture modes which control the breakup of tungsten alloys cylinders, and their influence on fragment morphology (see Sections 3.2 and 3.3 below).

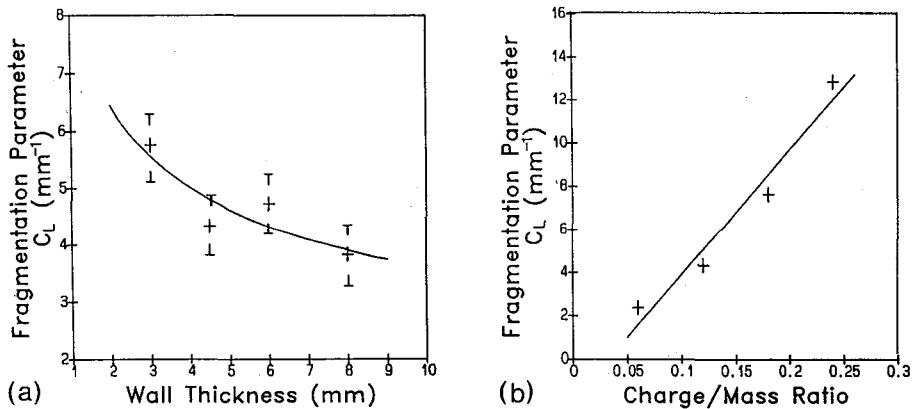


Fig.2 Variation of normalized Payman fragmentation parameter ( $C_L$ ) with (a) wall thickness ( $C/M = 0.12$ ) and (b) C/M ratio (wall thickness = 4.5mm), for Mass Range 1 fragments only. (Similar trends were observed for fragments from Mass Range 2.)

### 3.2 Fragment Fracture Modes

Macroscopic examination of representative samples of fragments using low-power optical microscopy revealed a number of important differences between tungsten alloy fragments and those derived from the ferrous alloys conventionally used in HE munitions [6]. The tungsten alloy cylinders experienced breakup predominantly by radial tensile fracture (see Fig.3 below). In contrast to the behaviour of cylinders made from ferrous alloys, full-wall shear along the longitudinal fracture surfaces was not observed on fragments from any of the cylinders tested. A significant number of fragments showed no shear fractures, particularly on their transverse fracture surfaces. Shear fractures adjacent to the original inner surfaces of the cylinders represented only a small percentage of total cylinder wall thickness at breakup. For example, for cylinders of constant C/M ratio (0.12), the proportions of shear fracture decreased from about 8% to 2% as wall thickness increased from 3 to 8 mm. With increasing C/M ratio (4.5 mm wall thickness), the proportions of shear fracture remained relatively constant at about 5% of cylinder wall thickness at breakup.

The low proportions of shear fracture observed can be ascribed to two factors. First, the high density of the tungsten alloy ( $17.2 \text{ Mg/m}^3$ ) resulted in cylinders of relatively low C/M ratio. Previous studies using ferrous alloys [7] have demonstrated a trend to lower proportions of shear fracture with decreasing C/M ratio. This effect results from the fact that as the cylinders expand, a zone of high compressive stress extends further from the inner cylindrical surface and is maintained for a longer duration, as C/M ratio is increased. Second, the tungsten alloy investigated had relatively low toughness at the strain rates generated by explosive loading. Consequently, radial tensile fractures were initiated relatively early during cylinder expansion, and propagated through most of the cylinder wall before breakup was completed by shear fractures to the inner cylindrical surface.

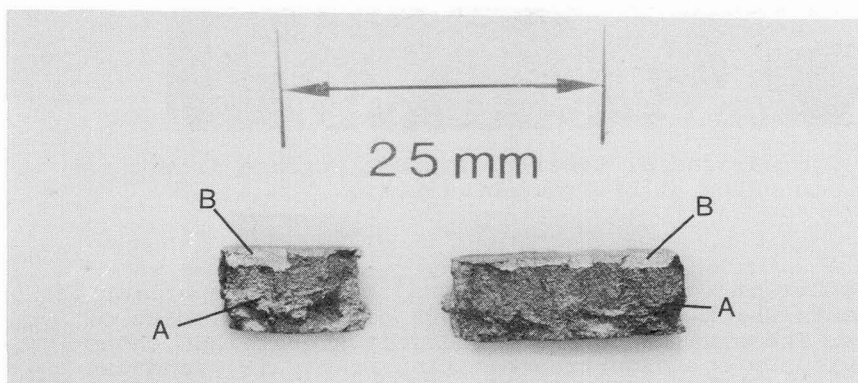


Fig.3 Typical fracture surfaces of tungsten alloy fragment showing longitudinal radial tensile fracture surface (A) and shear lip (B). (Note :top surface is inner wall) 2X

Fracture surfaces of representative fragments from each cylinder were examined using a Scanning Electron Microscope (SEM). Radial tensile fractures occurred predominantly by intergranular fracture between individual grains, with a smaller proportion of transgranular fracture (Fig. 4). Failure of the binder phase occurred predominantly by microvoid coalescence. Although there were differences in the proportions of the different fracture modes between individual cylinders, no clear trends could be identified with variations in cylinder wall thickness or C/M ratio.

### 3.3 Fragment Morphology

Because of the relatively large number of fragments (up to 6000) produced by some cylinders, a representative (10%) sample was selected at random from each fragment collection for fragment classification and measurement. Following the convention adopted in earlier studies [8], fragments were classified according to the proportions of inner and outer cylinder wall that was present. B-type (primary) fragments exhibited portions

of both the inner and outer surfaces of the cylinders from which they originated.

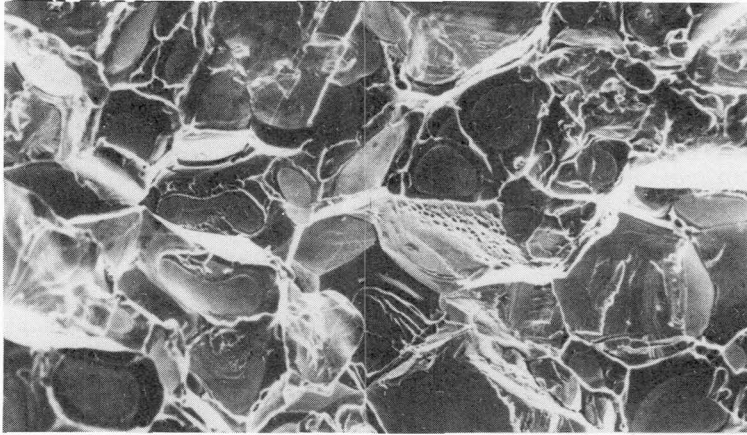


Fig.4 Typical radial tensile fracture surface from tungsten alloy fragment (900X).

A notable feature of this examination was the high proportion of B-type fragments which represented 60-80% of the total mass of all cylinders. These values are considerably higher than those reported previously for high-fragmentation steels [9], and can be ascribed to the predominance of radial tensile fracture discussed in Section 3.2 .

Table 3 summarizes measurements of B-type fragment widths, lengths and the percentage reductions in cylinder wall thickness at breakup. The average values of B-type fragment length and width are of crucial importance in the design of effective grids to control the breakup of metal casings into fragments of chosen mass and shape. In essence, they set the upper limits to the dimensions of an effective notching system.

Table 3  
Average Dimensions of B-type (Primary) Fragments

Cylinder Size	Wall Thick.	Average Dimensions of B-type Fragments			
		Length(mm)	Width(mm)	L/W Ratio	%REDN
1	8	9.3	3.3	2.8	14.1
2	6	6.6	2.0	3.3	13.8
3	4.5	6.3	1.9	3.3	14.3
4	3	4.8	1.3	3.7	13.1
5	4.5	5.0	1.7	2.9	13.2
6	4.5	6.2	1.7	3.6	15.1
7	4.5	7.3	1.6	4.6	13.5

Note: %REDN refers to percentage reduction in wall thickness of cylinders at breakup as measured on B-type fragments.

As observed in all cylindrical specimens (and munitions), the length of B-type fragments exceeds their width due to the much greater strains generated circumferentially rather than axially by explosive loading. Longitudinal fractures, particularly in relatively brittle materials, propagate essentially parallel to the longitudinal axis of the cylinder. In these experiments, length/width ratios were found to decrease slightly (3.7 - 2.8) with increasing wall thickness for cylinders of constant C/M ratio (0.12). With increasing C/M ratio (constant wall thickness), B-type fragment L/W ratios decreased from 4.6 to 2.9. Previous studies using steel cylinders of similar dimensions have demonstrated that L/W ratios of about 3 are invariably associated with alloys which produce very high  $C_L$  values [10].

There were no clear trends in reduction of thickness values (Table 3) measured on B-type fragments with variation in either cylinder wall thickness or C/M ratio. The majority of cylinders showed reduction of thickness values of approximately 13 - 14% which are similar to those determined for ferrous alloys which produce very fine fragment mass/number distributions, such as isothermally transformed HF-1 steel [8].

#### 3.4 Microstructural Features.

The microstructure of the as-received tungsten alloy cylinders consisted of recrystallised equi-axed tungsten particles within a W-Ni-Fe matrix. Examination of fragment cross-sections showed that adjacent to the inner cylindrical surfaces and extending inwards to approximately the depth of the shear zone, the tungsten particles are elongated into an elliptical form in the direction of maximum strain (circumferentially). A high density of deformation twins is generated in this region. In the middle and outer parts of fragments, the microstructure of the tungsten particles remains equi-axed, and the density of deformation twins decreases with distance from the inner cylindrical surface.

The nominal as received hardness of the tungsten alloy cylinders was 320HV30. Following detonation of the cylinders fragment hardness measurements increased to a maximum near the inner cylinder surface (of the order of 400 - 470 HV30), decreasing to a plateau value towards the centre of the cylinder wall thickness.

#### 4. CONCLUSIONS

For Composition B filled cylinders made from the W-Ni-Fe alloy investigated:

(a) Natural fragmentation behaviour cannot be accurately described by the conventional modified Payman mass/number distribution. However, the fragmentation of the alloy can be accurately represented using a dual slope linear fit to the modified Payman distributions determined for these cylinders.

(b) Tensile fracture dominates the breakup of these cylinders,



with shear fracture constituting less than 10% of cylinder wall thickness at breakup.

(c) Fragment classifications and measurements have established the baseline data for efficient design of notching systems to control the breakup of casings made from this alloy into fragments of preferred size.

## 5. REFERENCES

1. Craig B.G. et al, "High Density Metals and Metallic Composites for Improved Fragmentation Submunitions", Los Alamos Scientific Laboratory Report LA 6069-MS, New Mexico, December 1975.
2. Bedford A.J. and Krauklis P. "Fragmentation Data Analysis and Effects of Errors on Mass and Number Distributions", MRL Report 666, Melbourne, Australia, May 1976.
3. Burman N.M. "Simplification and Refinement of a Fragmentation Prediction Technique", MRL Report 804, Melbourne, Australia, 1981 (RESTRICTED).
4. Reid W.D. and Walsh B.E. "Fragmentation Scaling Relationships and Fracture Characterisation of Tungsten alloy Cylinders", MRL Technical Note 547, Melbourne, Australia, November 1976.
5. Walsh B.E. and Burman N.M. "Comparative Fragmentation of As-Cast and Ferritize-Annealed SG Iron Cylinders", MRL Report 1118, Melbourne, Australia, May 1988.
6. Clark E.N. "A Study of Fragmentation Mechanics", Fragmentation Technology Seminar, Picatinny Arsenal, Dover, USA, October 1969.
7. Walsh B.E. "The Influence of Geometry on the Natural Fragmentation of Steel Cylinders", MRL Report 533, Melbourne, Australia, January 1973.
8. ----- "Final Report on a Co-operative Research and Development Project between the Australian Department of Defence and the US Department of the Army on "Fracture Mechanisms in Naturally Fragmenting Materials", Report MOU/FM/1/75, October 1975.
9. Walsh B.E. "Comparison of Natural Fragmentation Scaling Behaviour of HF-1 and AISI 1045 Steel Cylinders using Normalized Payman Parameters", MRL Report 941, Melbourne, Australia, October 1984 (RESTRICTED).
10. Walsh B.E. "An Assessment of the Natural Fragmentation of Several Candidate Materials for the Production of 81 mm Mortar Bomb Casings", MRL Report 677, Melbourne, Australia, November 1976, (RESTRICTED).